AGU PUBLICATIONS

JGR

Journal of Geophysical Research: Atmospheres

RESEARCH ARTICLE
10.1002/2016JD025619

Key Points:
- An empirical algorithm is obtained to correlate nucleation rates with relative acidity, relative humidity, and temperature
- Our results imply that H_2SO_4-H_2O binary nucleation is negligible in the typical boundary layer temperature range (248–298 K)
- Collision-limited condensation of H_2SO_4 molecules underestimates sub-3 nm growth rate at temperatures $<$293 K but overestimates at temperatures $>$293 K

Supporting Information:
- Supporting Information S1

Correspondence to:
H. Yu and S.-H. Lee,
hyu@nuist.edu.cn;
shanhu.lee@nsstc.uah.edu

Citation:
Yu, H., L. Dai, Y. Zhao, V. P. Kanawade, S. N. Tripathi, X. Ge, M. Chen, and S.-H. Lee (2017), Laboratory observations of temperature and humidity dependencies of nucleation and growth rates of sub-3 nm particles, *J. Geophys. Res. Atmos.*, *122*, doi:10.1002/2016JD025619.

Received 6 JUL 2016
Accepted 23 JAN 2017
Accepted article online 25 JAN 2017

Laboratory observations of temperature and humidity dependencies of nucleation and growth rates of sub-3 nm particles

Huan Yu[1], Liang Dai[1], Yi Zhao[1], Vijay P. Kanawade[2], Sachchida N. Tripathi[3], Xinlei Ge[1], Mindong Chen[1], and Shan-Hu Lee[4]

[1]School of Environmental Science and Engineering, Nanjing University of Information Science and Technology, Nanjing, China, [2]University Centre for Earth and Space Sciences, University of Hyderabad, Hyderabad, India, [3]Centre for Environmental Science and Engineering and Department of Civil Engineering, Indian Institute of Technology Kanpur, Kanpur, India, [4]Department of Atmospheric Sciences, University of Alabama in Huntsville, Huntsville, Alabama, USA

Abstract Temperature and relative humidity (RH) are the most important thermodynamic parameters in aerosol formation, yet laboratory studies of nucleation and growth dependencies on temperature and RH are lacking. Here we report the experimentally observed temperature and RH dependences of sulfuric acid aerosol nucleation and growth. Experiments were performed in a flow tube in the temperature range from 248 to 313 K, RH from 0.8% to 79%, and relative acidity (RA) of sulfuric acid from 6×10^{-5} to 0.38 (2×10^{7}–10^{9} cm^{-3}). The impurity levels of base compounds were determined to be $NH_3 < 23$ pptv (parts per thousand by volume), methylamine < 1.5 pptv, and dimethylamine < 0.52 pptv. Our results showed that low temperatures favor nucleation at fixed sulfuric acid concentration but impede nucleation when RA is fixed. It is also shown that binary nucleation of sulfuric acid and water is negligible in planetary boundary layer temperature and sulfuric acid ranges. An empirical algorithm was derived to correlate the nucleation rate with RA, RH, and temperature together. Collision-limited condensation of free-sulfuric acid molecules fails to predict the observed growth rate in the sub-3 nm size range, as well as its dependence on temperature and RH. This suggests that evaporation, sulfuric acid hydration, and possible involvement of other ternary molecules should be considered for the sub-3 nm particle growth.

1. Introduction

New particle formation (NPF) is a significant source of cloud condensation nuclei (CCN) in the atmosphere at the global scale [*Merikanto et al.*, 2009; *Yu and Luo*, 2009]. NPF takes place in various atmospheric environments from the boundary layer to the upper troposphere and lower stratosphere, from tropical to polar regions, and from rural biogenic environments to extremely polluted megacities [*Kanawade et al.*, 2012; *Kulmala et al.*, 2004; *Zhang et al.*, 2012]. Sulfuric acid-water (H_2SO_4-H_2O) particle formation has been studied for decades both experimentally and theoretically to investigate the role of H_2SO_4-H_2O binary homogeneous nucleation (BHN), with or without ions, in the NPF within or beyond the boundary layer [*Yu*, 2002; *Kirkby et al.*, 2011]. There are still exceptional cases like extremely cold polar or upper troposphere and lower stratosphere conditions, low preexisting aerosol loading or extremely high H_2SO_4 concentration in sulfur plumes where BHN could be important in producing new particles [*Dunne et al.*, 2016]. Direct measurements of the temperature and relative humidity (RH) dependencies of aerosol nucleation rates and growth rates in well-controlled laboratory conditions are required to better understand the NPF processes in the wide range of atmospheric conditions.

Only a few studies have investigated the temperature-dependent nucleation rates [*Wyslouzil et al.*, 1991; *Brus et al.*, 2011; *Kirkby et al.*, 2011; *Duplissy et al.*, 2016]. *Kirkby et al.* [2011] showed nucleation rates of neutral and ion-induced nucleation of H_2SO_4-H_2O at three different temperatures of 248, 278, and 293 K in the CERN Cosmics Leaving OUtdoor Droplets (CLOUD) chamber. They found that binary nucleation with galactic cosmic rays (i.e., ion-induced nucleation) within the warm boundary layer is negligible but proceeds at significant nucleation rates at 248 K and atmospheric [H_2SO_4] of 10^{7} cm^{-3}. More recently, *Duplissy et al.* [2016] measured pure binary nucleation rates by sulfuric acid and water for neutral and ion-induced pathways at 207 K–299 K in the CLOUD chamber, where ion cluster chemical composition measured with atmospheric pressure interface time-of-flight (APi-TOF) was used to identify binary versus ternary nucleation systems. Their results show

that nucleation rates increase with increasing RH and H_2SO_4 concentrations, while nucleation rates decrease with increasing temperatures at a fixed RH and H_2SO_4 concentration. *Duplissy et al*. [2016]'s results agree with quantum chemistry-normalized classical nucleation theory (CNT) [*Merikanto et al*., 2016], which suggests that nucleation mechanisms, and hence *J* dependencies on RH and H_2SO_4, differ in different temperature and $[H_2SO_4]$ ranges.

Due to rapid coagulation losses to preexisting particles, particle growth rates in the sub-3 nm size range are crucial for determining the contribution of NPF to CCN (typically 50–100 nm), but this initial growth process is not well understood. Growth rates due to H_2SO_4 have been typically estimated assuming a collision-limited condensation process [*Nieminen et al*., 2010]. However, laboratory experiments showed that the observed growth rates of sub-3 nm particles are not consistent with the predictions of collision-limited H_2SO_4 condensation [*Sipila et al*., 2010; *Wimmer et al*., 2015; *Lehtipalo et al*., 2016; *Ehn et al*., 2014; *Berndt et al*., 2014; *Tröstl et al*., 2016]. A recent study has shown that sub-3 nm particle growth rates can be enhanced up to 1 order of magnitude higher by stabilizing base compounds like dimethylamine [*Lehtipalo et al*., 2016]. Recent laboratory measurements have shown that highly oxygenated organics not only participate in nucleation but also assist postnucleation growth [*Ehn et al*., 2014; *Berndt et al*., 2014; *Tröstl et al*., 2016]. In addition, growth rates are affected by H_2SO_4 evaporation at high temperatures [*Wimmer et al*., 2015].

Water is the other important precursor in H_2SO_4-H_2O BHN. While water is far more abundant and volatile than H_2SO_4 in the atmosphere, water stabilizes transitional clusters [*Vaida*, 2011] to increase nucleation rates. Calculations have also shown that the growth rate due to condensation of H_2SO_4 attached to three water molecules is higher by approximately 40% than that of unhydrated free-H_2SO_4 molecules [*Nieminen et al*., 2010].

Here we investigated the dependence of nucleation and growth rates on H_2SO_4 vapor concentration, RH and temperature using a flow tube reactor. We developed an empirical nucleation algorithm, based on these observations, to correlate the nucleation rate with the relative acidity (RA; saturation ratio) of H_2SO_4, RH, and temperature. We also examined how the observed growth rates of sub-3 nm particles deviate from those predicted from the collision-limited H_2SO_4 condensation under different temperatures and RH conditions.

2. Methods

2.1. Experimental Setup

The flow tube was constructed based on *Young et al*. [2008]; *Benson et al*. [2008], and *Yu et al*. [2012]. It consists of two components: a H_2SO_4 generator with OH photolysis and a temperature-controlled nucleation tube (Figure S1). In the H_2SO_4 generator OH radicals were produced from photodissociation of water vapor in a quartz tube illuminated by a mercury lamp (Pen-Ray Model 11SC-1, 185 nm wavelength selected by a band-pass filter Andover 193FS15). The quartz tube and the lamp were housed in a temperature-regulated enclosure, where nitrogen gas flowed through. The illumination area inside the enclosure was adjusted precisely, by moving the position of a dark tube using a linear actuator (Oriental Motor Model DRL60). The photon flux emitted from the lamp was monitored with a CsI phototube (Hamamatsu Model R5764). A flow of SO_2, O_2, and N_2 gas mixture merged with OH radicals, immediately after water vapor exited the illumination area. There was some CO impurities in the carrier nitrogen gas (99.9999%) vaporized from the liquid nitrogen, estimated to be less than 400 ppbv. The reaction rate coefficient of $CO + OH \rightarrow CO_2 + H$ ($2.4 \times 10^{-13}\,cm^{-3}\,s^{-1}$) is nearly a factor of 6 lower than that of $SO_2 + OH \rightarrow HSO_3$ ($1.5 \times 10^{-12}\,cm^{-3}\,s^{-1}$) at 298 K [*Seinfeld and Pandis*, 2006]. Therefore, the majority of OH (86%–92%) would react with SO_2 (0.5–1 ppmv).

Computational fluid dynamics analysis using ANSYS FLUENT 15.0 showed that a turbulence zone was created after the injection of $SO_2/O_2/N_2$ flow and distributed H_2SO_4 uniformly in the second half part of the H_2SO_4 generator. The Chemical Ionization Mass Spectrometer (CIMS) was not connected to the nucleation tube for direct H_2SO_4 measurement during the experiments. This arrangement was made to reduce the total flow rate (i.e., 4–7 standard liters per minute (sLpm)). When the H_2SO_4 flow entered the nucleation tube, there was turbulence within the first 10 cm of the 94 cm long nucleation tube. Then through the majority of the flow tube (84 out of 94 cm length), the flow was laminar (Reynolds number: 67–130).

The $[H_2SO_4]$ was calculated from the OH concentration ([OH]), assuming that the majority of OH radicals were converted to H_2SO_4 as discussed above:

$$[H_2SO_4] = I_{185nm}\sigma_{H_2O}\varphi_{OH}[H_2O]\times\Delta t \quad (1)$$

$[H_2SO_4]$ was adjusted by varying the position of the dark tube (hence, Δt) and the water vapor concentration $[H_2O]$. The water vapor concentration ($[H_2O]$, cm^{-3}) was monitored with a dew point hygrometer (Vaisala, Drycap® DMT242) and calculated as the following:

$$[H_2O] = \frac{6.02\times10^{17}P_d}{RT} \quad (2)$$

where P_d is water saturation vapor pressure (Pa) at the dew point and T is the flow tube temperature (K). $I_{185\ nm}\Delta t$ is the product of the light photon flux and the illumination time Δt and is obtained from the calibration using O_2 to O_3 actinometry $\left(I_{185nm}\Delta t = \frac{[O_3]}{[O_2]\sigma_{O_2}\varphi_{O_3}}\right)$ prior to the nucleation/growth experiments. This way, the determination of absolute photon flux was not needed. Error sources of the estimated $[H_2SO_4]$ include: (i) the UV lamp photon intensity shift and the oxygen absorption cross section variation (±25%), (ii) the linear actuator position repeatability determined from run-to-run experiments of the O_2 to O_3 actinometry (±10%), (iii) the dew point hygrometer uncertainty (±5%), and (iv) possible OH lost to CO (as opposed to reacting with SO_2) in the flow tube (8–14%). Thus, the overall uncertainty of the H_2SO_4 calibration was estimated to be ±30%.

Figure S2 shows the $[H_2SO_4]$ measured with the nitrate CIMS at the exit of H_2SO_4 generator versus the $[H_2SO_4]$ calculated from the O_2 to O_3 actinometry calibration. The uncertainty associated with CIMS measurements was estimated to be ±60% [*Erupe et al*., 2010; *Young et al*., 2008]. At higher $[H_2SO_4]$, CIMS signals were significantly lower than the calibrated values, likely because $[H_2SO_4]$ was approaching the upper limit of the CIMS detection. The agreement is reasonable when considering the uncertainties in two entirely independent methods.

The nucleation tube temperature was varied within 248–313 K with a circulating bath using ethanol as the working fluid. This temperature range covers the range of boundary layer temperature conditions. Before entering the nucleation tube, the main carrier gas flowed through a coiled stainless steel tube that was immersed in the circulating bath. This preheated or precooled carrier gas partly compensated for the temperature gradient at the beginning of nucleation tube. We probed the temperatures along the tube axis and found that the temperature at the 5 cm into the nucleation tube was within 2°C of the desired temperatures. To adjust the RH in the nucleation tube, nitrogen gas was flowed through deionized water in a water bubbler before entering the flow tube. Another dew point hygrometer measured the water vapor concentration at the exit of the nucleation tube (Figure S1).

An nCNC counter (also known as particle size magnifier, PSM; Airmodus A20) [*Vanhanen et al*., 2011] was attached to the exit of the nucleation tube. The nCNC was operated in a scanning mode with a cycle of 240 steps between the saturator flow rates from 0.1 to 1.0 sLpm within 240 s. The particle cutoff size of nCNC is dependent on the saturator flow rate. For example, at a saturator flow of 0.1 and 1.0 sLpm, the cutoff sizes are 2.94 nm and 1.38 nm, respectively. An inversion method based on *Lehtipalo et al*. [2014] and *Yu et al*. [2016] was used to obtain the particle size spectra (time resolution 4 min) in six size bins: 1.4–1.6, 1.6–1.9, 1.9–2.2, 2.2–2.4, 2.4–2.7, and 2.7–3.0 nm. The inverted particle number concentrations in these six bins were referred as $N_{1.5}$, $N_{1.8}$, $N_{2.0}$, $N_{2.3}$, $N_{2.6}$, and $N_{2.8}$, respectively. The residence time varied from 45 to 70 s in the nucleation tube. Under these conditions, the majority of nucleated particles did not grow to larger than 3 nm. That is, particle counts at a saturator flow rate of 0.1 sLpm (PSM measures particles larger than 3.0 nm) were less than 10% of particles counts at 1.0 sLpm (particles larger than 1.4 nm). Even at the lowest sample flow temperature (248 K), background particles generated via homogeneous nucleation from the working fluid (DEG) were negligible. At different sample flow temperatures, the growth tube and inlet temperatures of nCNC were kept constant. Therefore, the cutoff size of the nCNC did not change at different experimental conditions.

One of the common issues in nucleation experiments is that there are always unavoidable impurities of base compounds (e.g., ammonia and amines) present in the nucleation reactor or chamber [*Yu et al*., 2012; *Almeida et al*., 2013; *Jen et al*., 2014; *Kirkby et al*., 2011; *Zollner et al*., 2012; *Bianchi et al*., 2014; *Duplissy et al*., 2016; *Glasoe*

et al., 2015]. Base compounds, even at the sub-pptv (parts per thousand by volume) level can affect H_2SO_4-H_2O nucleation rates [*Almeida et al*., 2013; *Jen et al*., 2014; *Glasoe et al*., 2015]. We produced particles from H_2SO_4 and water vapor, while base compounds like amines or ammonia were not introduced throughout the experimental period. The impurity concentrations of the ammonia (NH_3) and amines were determined with offline analytical methods: high-performance liquid chromatography (HPLC) and ion chromatography (IC). The impurity NH_3, methylamine, and dimethylamine mixing ratios were below 23 pptv, 1.5 pptv and 0.52 pptv, respectively. Text S1 in the supporting information describes how we minimized and quantified the concentrations of base impurities.

2.2. Determination of Nucleation Rate and Growth Rate

We obtained both nucleation rates and growth rates from our flow tube experiments. Growth rates in a nucleation chamber have been determined from the observed time evolution of maximum concentrations (or half maxima) in successive size bins using particle instruments such as PSM, Neutral Air Ion Spectrometer (NAIS), or Condensation Particle Counter (CPC) battery [*Kulmala et al*., 2012; *Lehtipalo et al*., 2014]. Alternatively, growth rates were calculated from the observed particle size distributions at a known residence time in a flow tube by varying $[H_2SO_4]$ [*Sipila et al*., 2010]. In the present flow tube study, we used the latter method.

H_2SO_4 vapor was produced as a point source at the entrance of the nucleation tube. Wall loss in the laminar flow of the nucleation tube was quantified as the following [*Young et al*., 2008]:

$$[H_2SO_4]_t = H_2SO_4]_0 e^{-k_L t} \tag{3}$$

where $[H_2SO_4]_0$ and $[H_2SO_4]_t$ are the initial concentration and the concentration after time t in the nucleation tube, respectively. k_L is the diffusion-limited wall loss coefficient [*Hanson and Eisele*, 2000]:

$$k_L = 3.65D/r^2 \tag{4}$$

where r is the radius of the nucleation tube and D is the diffusion coefficient. Humidity- and temperature-dependent D was calculated from *Hanson and Eisele* [2000]. The maximum loss of H_2SO_4 to particles can be estimated by comparing particle mass concentration at the exit of the nucleation tube and $[H_2SO_4]_0$ at the entrance. Assuming that all particles were 2 nm diameter spheres composed only of pure H_2SO_4 with density of 1.84 g cm^{-3}, at most 4.4% of H_2SO_4 molecules were depleted by particle formation, neglecting water and other possible molecules in the particles. If considering the diffusional loss of H_2SO_4 to the wall was 55–80% for the given residence time, H_2SO_4 loss onto particles was neglected in further analysis of this study. The same treatment was made in recent nucleation flow tube studies like *Young et al*. [2008], *Skrabalova et al*. [2014], *Neitola et al*. [2015], and *Brus et al*. [2016].

Particle growth rate GR_t at time t in the nucleation tube is related to $[H_2SO_4]_t$ via

$$GR_t = \frac{dD_p}{dt} = k_{G,obs}[H_2SO_4]_t/10^7 cm^{-3} \tag{5}$$

Here the observed growth rate factor due to 10^7 cm^{-3} H_2SO_4 monomer ($k_{G,obs}$) was assumed to be constant within 1–3 nm. From equations (3)–(5), diameter change $\Delta D_{p,t_r}$ after a residence time t_r is integrated as the following:

$$\Delta D_{p,t_r} = \int_0^{t_r} k_{G,obs}[H_2SO_4]_t/10^7 cm^{-3} dt = k_{G,obs}[H_2SO_4]_0/10^7 cm^{-3} \frac{1 - e^{-k_L t_r}}{k_L} \tag{6}$$

Rearranging equation (6) yields

$$k_{G,obs} = \frac{\Delta D_{p,t_r} \times 10^7 cm^{-3}}{[H_2SO_4]_0} \frac{k_L}{1 - e^{-k_L t_r}} \tag{7}$$

By varying $[H_2SO_4]_0$ at the entrance of the nucleation tube, particles with different mean diameter $D_{p,mean}$ were generated at the exit of the nucleation tube (Figure 1). $D_{p,mean}$ was calculated from

$$D_{p,mean} = \sum N_i D_{p,i} / \sum N_i \tag{8}$$

where N_i is the particle number concentration in each size bin i (i = 1–6) and $D_{p,i}$ is the mean diameter in the size bin i. The particle mean diameter $D_{p,mean}$ represents the sum of the critical cluster diameter and

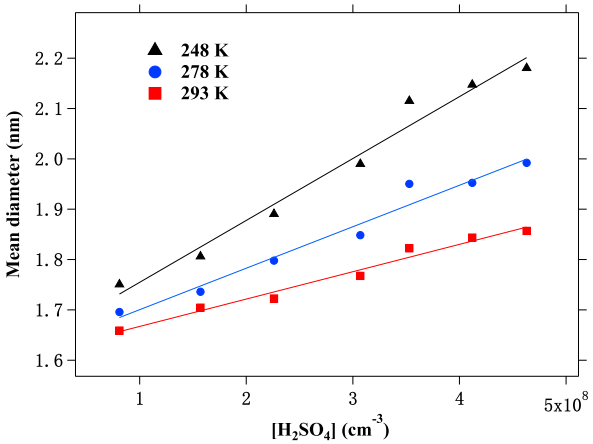

Figure 1. Particle mean diameter $D_{p,\mathrm{mean}}$ measured at the exit of the nucleation tube, as a function of initial H_2SO_4 concentration $[H_2SO_4]_0$ and temperature. Residence time was 60 s. Water vapor pressure was fixed at 62 Pa (1.5×10^{16}–1.8×10^{16} cm^{-3}). The error in diameter was estimated to be in the order of ±0.2 nm for inorganic ions. $[H_2SO_4]$ uncertainty was estimated to be ±30%.

the net particle growth after nucleation ($\Delta D_{p,t_r}$). Figure 1 shows a clear linear correlation between $D_{p,\mathrm{mean}}$ and $[H_2SO_4]_0$ at all three temperatures. The intercepts at the diameter axis correspond to the critical size of 1.7 ± 0.1 nm, equivalent to the volume diameter of ~1.4 ± 0.1 nm [*Larriba et al.*, 2011], which are consistent with estimates from other studies [*Kulmala et al.*, 2013]. Here we assumed that the critical size was not very sensitive to H_2SO_4 or RH changes in our study. The critical size variability may not be detectable, given the accuracy of our PSM measurement. The slope of the linear fitting equal to $\frac{\Delta D_{p,t_r}}{[H_2SO_4]_0}$ in equation (7). Therefore, $k_{\mathrm{G,obs}}$ can be obtained from the product of the slope and the term $\frac{k_L\times10^7\,cm^{-3}}{1-e^{-k_L t_r}}$. For the $[H_2SO_4]$ range from 8×10^7 to 5×10^8 cm^{-3} (Figure 1), k_G was derived to be 1.07 to 0.58 nm h^{-1} for temperatures between 248 and 293 K.

The uncertainty of $k_{\mathrm{G,obs}}$ in equation (7) comes from (1) the uncertainty of H_2SO_4 measurement (±30%) and (2) the uncertainties of $D_{p,\mathrm{mean}}$ and mean particle residence time in the nucleation tube. The error in diameter was determined to be in the order of ±0.2 nm (or ± 12%) for inorganic ions [*Lehtipalo et al.*, 2014, 2016; *Kulmala et al.*, 2013]. Our H_2SO_4 wall loss analysis estimated that 83% of particles were nucleated in the first half of the nucleation tube. The mean residence time t_r of these particles was within 30% less than the flow residence time (45–70 s). Considering the uncertainties of $[H_2SO_4]$, $\Delta D_{p,t_r}$, and t_r, we estimated that the uncertainty of $k_{\mathrm{G,obs}}$ in equation (7) was ± 40%.

The nucleation rate is dependent on $[H_2SO_4]$ which decays in the nucleation tube following equation (3). Considering H_2SO_4 as the controlling precursor, the nucleation rate at time t (J_t) can be expressed as

$$J_t = k_N[H_2SO_4]_t^n = J_0 e^{-nk_L t} \tag{9}$$

J_0 is the initial nucleation rate in the nucleation tube at the initial H_2SO_4 concentration $[H_2SO_4]_0$. The total particle number concentration observed at the exit of nucleation tube can be calculated from

$$N_{\mathrm{tot}} = \int_0^{t_r} J_t dt = J_0 t_r \frac{1-e^{-nk_L t_r}}{nk_L t_r} \tag{10}$$

Given t_r = 45–70 s, k_L = 0.014–0.02 s^{-1}, and n = ~3, the term $e^{-nk_L t_r}$ can be neglected, which leads to the following approximation:

$$N_{\mathrm{tot}} \approx \frac{J_0}{nk_L} = \frac{k_N[H_2SO_4]_0^n}{nk_L} \tag{11}$$

We obtained the nucleation theorem power n from linear fitting between Log N_{tot} and Log$[H_2SO_4]_0$ $\left(\text{that is, } n = \frac{\Delta \log N_{\mathrm{tot}}}{\Delta \log [H_2SO_4]_0}\right)$. The n varied from 2.8 to 3.5 between different experiment sets. Then J_0 was calculated from the product $N_{\mathrm{tot}} \times nk_L$. To evaluate the dependence of nucleation rate on H_2SO_4, we used $[H_2SO_4]_0$ and J_0 in this work (not the average nucleation rate from N_{tot}/t_r). The critical size of nucleation was ~1.7 nm from our flow tube experiments, as shown earlier (Figure 1). Thus, the particles in the first size bin of 1.4–1.6 nm (2×10^2 to 3×10^3 cm^{-3} or 3–21% of the total number concentration) were regarded as prenucleation clusters. N_{tot} was calculated from the sum of the other five bins ($N_{1.8}$, $N_{2.0}$, $N_{2.3}$, $N_{2.6}$, and $N_{2.8}$). Uncertainties of the estimated J_0 were from the following: (i) the statistical error of N_{tot} between run-

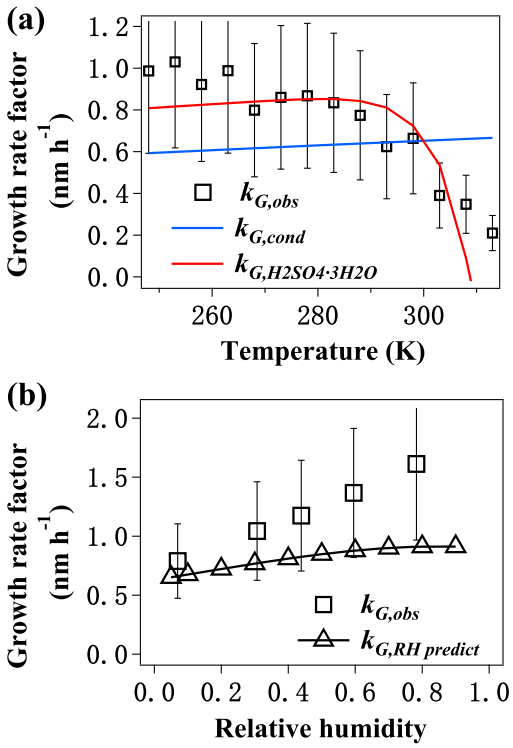

Figure 2. (a) A comparison of the observed growth rate factor of H_2SO_4 over sub-3 nm particles ($k_{G,meas}$, black squares) with the collision limited of condensation of free H_2SO_4 molecules ($k_{G,cond}$, blue curve) and evaporation-corrected growth rate factor of $H_2SO_4 \cdot 3H_2O$ ($k_{G,H_2SO_4 \cdot 3H_2O}$, red curve) at 248–313 K. Water vapor pressure was fixed at 62 Pa and $[H_2SO_4]$ ranged from 8×10^7–5×10^8 cm^{-3} during the growth rate measurements. (b) A comparison between the observed $k_{G,meas}$ (squares) for RH between 6% and 79% and RH-dependent condensational growth rate factor ($k_{G,RH\ predict}$, triangles) predicted by *Nieminen et al.* [2010] using H_2SO_4-hydrate distribution data. Temperature was fixed at 298 K.

to-run experiments (±20%), which was likely due to PSM counting noises and inversion uncertainties [*Lehtipalo et al.*, 2014], (ii) the k_L uncertainty (±7%) [*Hanson and Eisele*, 2000], and (iii) the omission of e^{-nk_Lt} in equation (11) (up to 16%). The overall uncertainty of J_0 was ± 27%.

3. Results

3.1. Temperature-, H_2SO_4-, and Humidity-Dependent Growth Rates

In Figure 2a we compared our observed growth rate factor ($k_{G,obs}$) at 248–313 K and a fixed water vapor pressure (62 Pa; corresponding vapor concentration 1.5×10^{16}–1.8×10^{16} cm^{-3}) with the theoretical growth rate factor ($k_{G,cond}$) due to collision-limited condensation of $10^7 cm^{-3}$ H_2SO_4 in the 1–3 nm size range. $k_{G,cond}$ was calculated following equation (8) of *Nieminen et al.* [2010]. It was noted that our observed $k_{G,obs}$, the apparent growth rate, may also include the contribution of particle self-coagulation [*Leppä et al.*, 2011; *Kontkanen et al.*, 2016]. The nucleation mode growth rate due to self-coagulation can be calculated using an analytical resolution by *Stolzenburg et al.* [2005]. Assuming an average size of 2 nm and particle number concentration of 10^4 cm^{-3}, we estimated that the growth rate due to self-coagulation is ~0.01 nm h^{-1}. This is negligible in the observed apparent growth rate, which is in the order of tens of nm h^{-1}.

We find that $k_{G,cond}$ and $k_{G,obs}$ are within the same order of magnitude, but they have opposite temperature dependencies. When the temperature increased from 248 to 313 K, $k_{G,cond}$ increased slightly from 0.6 to ~0.7 nm h^{-1}, whereas $k_{G,obs}$ decreased dramatically from ~1 to 0.3. Our results were very similar to that published by *Wimmer et al.* [2015], although the focuses of these two studies were different. Therefore, the collision-limited condensation underestimates H_2SO_4 growth rate at low temperatures (<293 K) but overestimates at high temperatures (>293 K). The deviations most likely result from two factors: (1) evaporation of H_2SO_4 at high temperatures and (2) other secondary or ternary species (like water and possibly base compounds) that assist the growth of sub-3 nm particles at low temperatures. A correction factor $f(T)$ was derived from our experimental results to correct the GR deviation from the collision-limited H_2SO_4 condensation:

$$GR = f(T)^* k_{G,cond}[H_2SO_4]/10^7 cm^{-3} \quad (12)$$

where $f(T) = -0.019\,T + 6.552$. Note that these experimentally derived growth rate factors were obtained at a fixed water vapor pressure (62 Pa) and a specific range of $[H_2SO_4]$ (8×10^7–5×10^8 cm^{-3}).

To evaluate the effect of evaporation and water condensation on the H_2SO_4 growth rate, we further calculated the evaporation-corrected $k_{G,H_2SO_4 \times 3H_2O}$ of $H_2SO_4 \cdot 3H_2O$ [*Nieminen et al.*, 2010]:

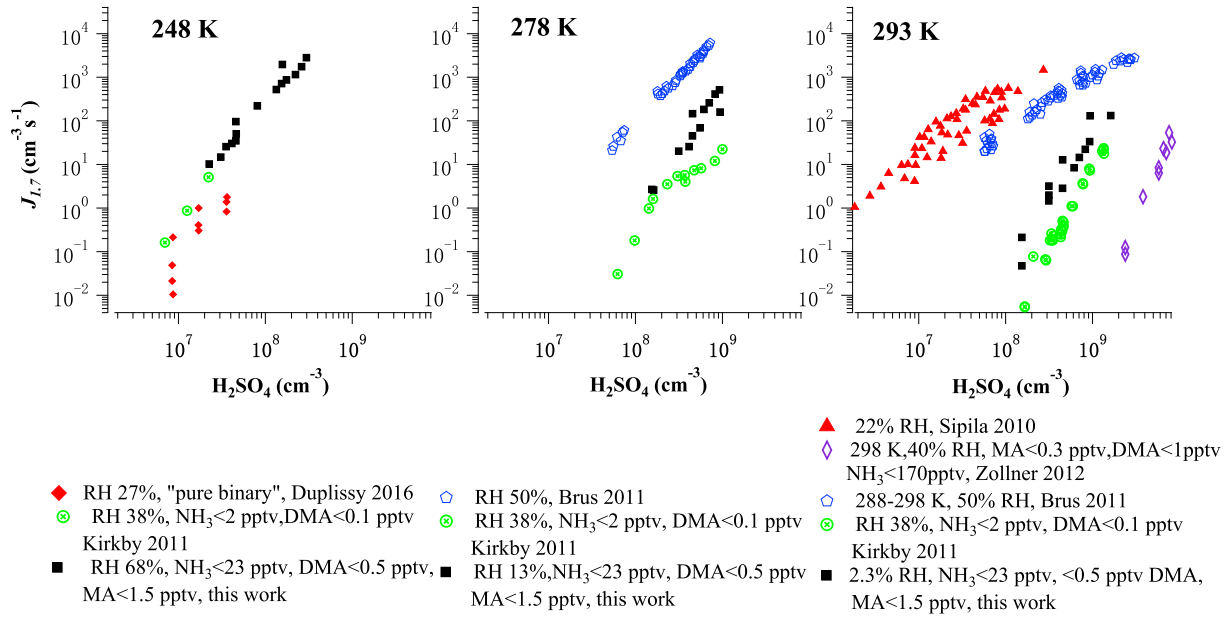

Figure 3. A comparison of this work with previous laboratory studies of temperature-dependent H_2SO_4-H_2O nucleation rate measurements. RH and base impurity levels are annotated, where they are available. DMA: dimethylamine; MA: methylamine. Experiment chamber was exposed to galactic cosmic rays in *Kirkby et al.* [2011] and *Duplissy et al.* [2016]. Other experiments were conducted in flow tubes without removing ions. The J_0 uncertainties in this work were ±27%.

$$GR_{H_2SO_4\times 3H_2O} = \frac{\gamma}{2\rho_{v,H_2SO_4\cdot 3H_2O}}\left(1+\frac{D_{v,H_2SO_4\cdot 3H_2O}}{D_p}\right)^2\left(\frac{8kT}{\pi}\right)^{\frac{1}{2}}\left(\frac{1}{m_p}+\frac{1}{m_{v,H_2SO_4\cdot 3H_2O}}\right)^{\frac{1}{2}} \quad (13)$$
$$m_{v,H_2SO_4\cdot 3H_2O}\times\left([H_2SO_4]-[H_2SO_4]_{surface}\right)$$

$$k_{G,H_2SO_4\cdot 3H_2O} = GR_{H_2SO_4\cdot 3H_2O}\cdot 10^7/[H_2SO_4] \quad (14)$$

Here $[H_2SO_4]$ of 3×10^8 cm^{-3} was used (representative of the experimental range 0.8–5×10^8 cm^{-3}). $GR_{H_2SO_4\cdot 3H_2O}$ was calculated for 2 nm particles (an average of 1 and 3 nm). $[H_2SO_4]_{surface}$ is the H_2SO_4 concentration over the surface of a 2 nm particle, which is assumed to be composed of a binary solution of H_2SO_4 and water. The composition of the binary solution was estimated so that particle-phase water is in equilibrium with the water vapor in the gas phase (62 Pa). Saturation vapor pressures of pure water and H_2SO_4 were adapted from *Vehkamäki et al.* [2002] and the kinetic term in equation (13) from *Nieminen et al.* [2010]. As shown in Figure 2a, the corrected $k_{G,H_2SO_4\cdot 3H_2O}$ has a better agreement with $k_{G,obs}$, showing similar temperature dependencies. The differences between $k_{G,H_2SO_4\cdot 3H_2O}$ and $k_{G,obs}$ at low temperatures (<263 K) may be due to cocondensation of more water molecules or other ternary vapors such as NH_3 and amines.

When calculating the contribution of H_2SO_4 to growth rate, one should determine whether H_2SO_4 is bound to one, two, or three water molecules, depending on RH [*Nieminen et al.*, 2010]. In order to understand RH dependence of the H_2SO_4 growth rate, we measured $k_{G,obs}$ by varying RH from 6% to 79% at 298 K (Figure 2b). $k_{G,obs}$ is compared with the $k_{G,RH\ predict}$ predicted by *Nieminen et al.* [2010], which used the H_2SO_4-hydrate distribution at 298 K from *Kurtén et al.* [2007]. As shown in Figure 2b, $k_{G,obs}$ is more sensitive to RH than $k_{G,RH\ predict}$. While at low RH of 6% $k_{G,obs}$ is close to $k_{G,RH\ predict}$, at RH of 30% $k_{G,obs}$ approaches $k_{G,RH\ predict}$ with three water molecules. The further increase of $k_{G,obs}$ at RH >30% indicates that H_2SO_4 molecule is associated with more than three water molecules. In our previous study *Yu et al.* [2012] has shown that base impurities dissolved in deionized water in the water bubbler was the major contamination source in the flow tube. Therefore, we expect a higher concentration of base impurities at higher RH. The clustering of base molecules with H_2SO_4 could also be the reason of larger discrepancy between $k_{G,obs}$ and $k_{G,RH\ predict}$ at higher RH.

3.2. Temperature-, H_2SO_4-, and Humidity-Dependent Nucleation Rates

Our J_0 versus $[H_2SO_4]_0$ data are compared with previous laboratory studies involving the temperature dependence of binary nucleation rates [*Kirkby et al.*, 2011; *Sipila et al.*, 2010; *Brus et al.*, 2011; *Zollner et al.*, 2012;

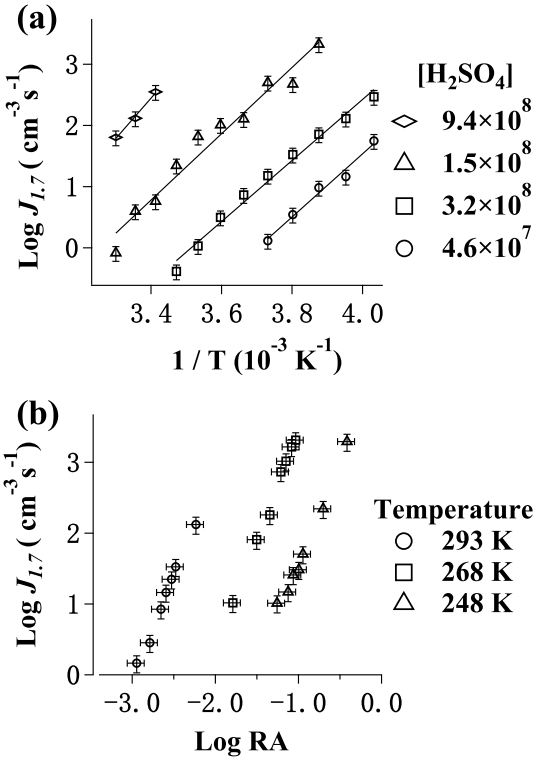

Figure 4. Log *J* versus 1/T for [H_2SO_4] of 4.6×10^7–9.4×10^8 cm^{-3} at the (a) water vapor pressure of 61 Pa, and the dependence of Log *J* on Log RA at three temperatures of 248, 268, and 293 K (b). The error bars are uncertainties associated with nucleation rate and [H_2SO_4] measurements.

Duplissy et al., 2016] in Figure 3. All these experiments used a PSM with cutoff diameters near the critical size, except that *Zollner et al*. [2012] used an ultrafine CPC. Among them, *Kirkby et al*. [2011], *Zollner et al*. [2012], and our work measured base impurity levels. *Duplissy et al*. [2016] obtained the "pure" binary nucleation rate at 249 K by excluding contaminated experiment runs based on the molecular identification of charged clusters using an APi-TOF. These experiments showed quite different nucleation rates, up to 4 orders of magnitude, at the same [H_2SO_4] levels. Such a difference could be due to measurement methods (e.g., chamber study versus flow tube study), impurity levels, and RH (annotated in Figure 3).

Our data are consistent with *Kirkby et al*. [2011] at the lowest temperature of 248 K. Given the same [H_2SO_4] at 278 and 293 K, our nucleation rate was within 20 times higher than *Kirkby et al*. [2011]. Or given the same nucleation rate, [H_2SO_4] was within about 1 order of magnitude between our study and *Kirkby et al*. [2011]. This discrepancy may be because of the cleaner conditions in the CLOUD chamber (e.g., NH_3 and dimethyalmine were <2 pptv and <0.1 pptv, respectively, in the CLOUD chamber [*Almeida et al*., 2013]). In addition, the different way of determining nucleation rates could be another source of uncertainty, e.g., initial nucleation rate at the beginning of fast flow nucleation tube versus nucleation rate derived from the time evolution of particle number concentrations in a large chamber. The slopes of log *J* versus log [H_2SO_4] in our experiments (2.8–3.1) at the three temperatures are within the range of 2.7–5.0 by *Kirkby et al*. [2011]. In contrast, the slopes of log *J* versus log [H_2SO_4] measured by *Brus et al*. [2011] and *Sipila et al*. [2010] ranged from 1.2 to 2.2 for temperature of 278–298 K. The slopes were <1 at 207 K in *Duplissy et al*. [2016]. This implies that nucleation in their work is kinetically limited, due to high concentration of stabilizing molecules [*Brus et al*., 2011] or low temperature [*Duplissy et al*., 2016].

Figure 4a shows log *J* versus 1/T at [H_2SO_4] of 4.6×10^7–9.4×10^8 cm^{-3} for the same water vapor pressure (61 Pa; corresponding water concentrations 1.5×10^{16}–1.8×10^{16} cm^{-3}). These results indicate that low temperatures favor nucleation at the same concentration of H_2SO_4, consistent with other studies [*Kirkby et al*., 2011; *Duplissy et al*., 2016; *Brus et al*., 2011]. The slopes of log *J* versus 1/T ranged from 4990 to 6000 for [H_2SO_4] of 4.6×10^7–9.4×10^8 cm^{-3}. Thus, the enhancement factor of *J* due to the temperature decrease was relatively constant independent of the [H_2SO_4] level.

It is thought that saturation ratio of nucleating vapor is more useful in determining nucleation rate than absolute vapor concentrations [*Ball et al*., 1999; *Glasoe et al*., 2015]. We calculated relative acidity (RA) and RH by dividing [H_2SO_4] and [H_2O] by saturation vapor concentrations of H_2SO_4 and water [*Vehkamäki et al*., 2002], respectively. Log *J* versus log RA was constructed in Figure 4b at 248 K, 268 K, and 293 K. For the same RA, the nucleation rate increased with the increasing temperature, in good agreement with *Wyslouzil et al*. [1991] and with the CNT predictions [*Seinfeld and Pandis*, 2006] which show that at the same saturation ratio an increasing temperature increases the exponential term of nucleation rates.

Note that the RH used in Figure 4b was not held constant, because we kept water vapor pressure constant (54 Pa) at different temperatures. To understand the effect of RA and RH on the nucleation rate, we conducted systematic measurements of nucleation rates under different RH (2.6%–79%), RA (6×10^{-4}–0.38), and T (248–298 K) conditions. Only one parameter (amongst $[H_2SO_4]_0$, $[H_2O]$, and T) was varied in each set of the experiments, while the others were fixed. In total, 134 sets of experiments were conducted. From multiple linear regression analysis on Ln J_0, Ln RA, Ln RH, and 1/T, we obtained the same form of the nucleation theorem. The multiple linear regression analysis led to the following expression ($R^2 = 0.894$ for $n = 134$):

$$J = 10^{41.8}[\mathrm{RA}]^3[\mathrm{RH}]e^{\frac{-2.4\times10^4}{T}} \quad (15)$$

The nucleation theorem power n for RA and RH is 3 and 1, respectively. It should be noted that the composition of the critical cluster, i.e., the number of molecules, cannot be derived directly from these theorem powers [*Ehrhart and Curtius*, 2013; *Kupiainen-Määttä et al*., 2014]. The positive correlation between the nucleation rate and the temperature is consistent with the observation that the nucleation rate increases with the increasing temperature for a certain RA (Figure 4b). The prefactor in the expression ($10^{41.8}$) in equation (15) is very likely dependent on the level of ternary nucleating species like NH_3, amines, or organic species. It is the first time, to the best of our knowledge, an experimental expression of nucleation rates was derived by simultaneously considering RA, RH, and temperature. The enhancement factor of the nucleation rate due to temperature changes can be directly calculated from equation (15). Equation (15) and Figure 4a imply that the enhancement factor due to the decreasing temperature is independent of $[H_2SO_4]$ (or RA) and RH. For a certain RH and $[H_2SO_4]$, a decrease of 10 K results in a nucleation rate enhancement factor of 3–8, depending on the temperature. A decrease of 20 K from 298 to 278 K resulted in a nucleation rate enhancement factor of ~10. This factor is quite close to those measured by *Brus et al*. [2011] at the same temperatures. In contrast, the enhancement between 207 K and 223 K measured by *Duplissy et al*. [2016] is weak. These observations support the predictions of quantum chemistry-normalized CNT [*Merikanto et al*., 2016], which show that under low temperatures (207–223 K) a barrierless kinetic nucleation can take place (hence, weak J dependence on temperature), whereas under high temperatures (>248 K) there is a Gibbs free energy barrier in nucleation (strong J dependence on temperature).

In this work we did not test the dependence of J on base compounds. Even though there were impurities of ternary nucleating vapors in the nucleation tube (i.e., $NH_3 < 23$ pptv, methylamine < 1.5 pptv and dimethylamine < 0.52 pptv), equation (15) indicates that 1.4×10^7–2×10^8 cm^{-3} H_2SO_4 was still required to produce atmosphere-relevant nucleation rates (>1 cm^{-3} s^{-1}) in the temperature range covering the planetary boundary layer (i.e., 248–298 K). Therefore, our experiments imply that binary nucleation is negligible in boundary layer conditions.

4. Conclusions

We have measured nucleation and growth rates of sub-3 nm particles produced from H_2SO_4 in a laminar nucleation tube. Experiments were conducted in the temperature range from 248 to 313 K, RH from 0.8% to 79%, and RA from 6×10^{-5} to 0.38. The observed slope of log J versus log $[H_2SO_4]$ did not vary much (2.8–3.5) for the temperature range from 248 to 298 K, while the slope of log J versus log $[H_2O]$ was close to 1. For the same RA and RH, higher temperatures are favorable for nucleation, as predicted from classical homogeneous nucleation theories. An algorithm of nucleation rate as the function of RA, RH, and temperature was derived on the basis of our experimental results (equation (15)).

The cluster size distribution measurements show that the nucleation critical cluster is around 1.7 ± 0.1 nm. Growth rates of sub-3 nm particles exhibit a linear correlation with $[H_2SO_4]$ for the $[H_2SO_4]$ range from 8×10^7 to 5×10^8 cm^{-3}, and the growth rate factor (GR/$[H_2SO_4]$) is dependent on temperature (equation (12), Figure 2a) and RH (Figure 2b). Collision-limited condensation of unhydrated H_2SO_4 molecules fails to predict such dependencies. Our results strongly suggest that the effects of evaporation, H_2SO_4 hydration, and other ternary molecules (like NH_3 and amines) must be considered in sub-3 nm particle growth.

Laboratory data with low and, more importantly, known impurity level are critical to obtain realistic parameterizations of particle formation rates for modeling purposes. In this study we overcame several problems associated with our previous flow reactor studies. HPLC and IC were used to measure the concentrations

of contaminant species (NH_3, methylamine, and dimethylamine), and experiments were done only when those species were below detectable levels. We used an up-to-date instrument PSM to count particles in the 1–3 nm range. Mathematical treatment was used to derive accurate nucleation rates and corresponding H_2SO_4 concentrations. The vast discrepancy of nucleation rates reported for binary systems in the past is now narrowed down considerably. Given the same nucleation rate, our [H_2SO_4] agrees now with *Kirkby et al*. [2011] and *Duplissy et al*. [2016] within about 1 order of magnitude. Recently, the dependence of binary nucleation rate on [H_2SO_4] and temperature (but not RH) was parameterized by *Dunne et al*. [2016] and fitted to CERN CLOUD measurements. However, it is the first time that an experimental expression of nucleation rates was derived in our study by simultaneously considering RA, RH, and temperature. The observation of sub-3 nm growth rates also added to the novelty of our study, as they have been studied far less than nucleation rates. Our study adds to the growing number of studies on nucleation and growth rates for the binary system of H_2SO_4 and H_2O and addresses the timely question of RH and T dependence of nucleation and growth rates.

Acknowledgments

This work was supported by National Science Foundation of China (grant 41405116 and 41675124); Natural Science Foundation of Jiangsu Province (grant BK20140989); the National Key Research and Development Program of China (2016YFC0203100); and the Jiangsu Specially Appointed Professor Grant. S.H.L. thanks NSF (AGS-1137821 and 1241498). We thank Robert McGraw of Brookhaven National Lab for his valuable suggestions in nucleation and growth rate determination. The authors comply with AGU's data policy and all data of this work could be obtained from H. Yu (hyu@nuist.edu.cn).

References

Almeida, J., et al. (2013), Molecular understanding of sulphuric acid-amine particle nucleation in the atmosphere, *Nature*, *502*(7471), 359–363, doi:10.1038/nature12663.

Ball, S. M., D. R. Hanson, F. L. Eisele, and P. H. McMurry (1999), Laboratory studies of particle nucleation: Initial results for H_2SO_4, H_2O, and NH_3 vapors, *J. Geophys. Res.*, *104*, 23,709–23,718, doi:10.1029/1999JD900411.

Benson, D. R., L. H. Young, R. Kameel, and S.-H. Lee (2008), Laboratory-measured sulfuric acid and water homogeneous nucleation rates from the SO_2 + OH reaction, *Geophys. Res. Lett.*, *35*, L11801, doi:10.1029/12008GL033387.

Berndt, T., M. Sipilä, F. Stratmann, T. Petäjä, J. Vanhanen, J. Mikkilä, and M. Kulmala (2014), Enhancement of atmospheric H_2SO_4/H_2O nucleation: Organic oxidation products versus amines, *Atmos. Chem. Phys.*, *14*(2), 751–764, doi:10.5194/acp-14-751-2014.

Bianchi, F., et al. (2014), Insight into acid-base nucleation experiments by comparison of the chemical composition of positive, negative and neutral clusters, *Environ. Sci. Technol.*, *48*, 13,675−13,684, doi:10.1021/es502380b.

Brus, D., K. Neitola, A. P. Hyvärinen, T. Petäjä, J. Vanhanen, M. Sipilä, P. Paasonen, M. Kulmala, and H. Lihavainen (2011), Homogenous nucleation of sulfuric acid and water at close to atmospherically relevant conditions, *Atmos. Chem. Phys.*, *11*, 5277–5287, doi:10.5194/acp-11-5277-2011.

Brus, D., L. Skrabalova, E. Herrmann, T. Olenius, T. Travnickova, and J. Merikanto (2016), Temperature-dependent diffusion coefficient of H_2SO_4 in air: Laboratory measurements using laminar flow technique, *Atmos. Chem. Phys. Discuss.*, *2016*, 1–26, doi:10.5194/acp-2016-398.

Dunne, E. M., et al. (2016), Global atmospheric particle formation from CERN CLOUD measurements, *Science*, *354*(6316), 1119–1124, doi:10.1126/science.aaf2649.

Duplissy, J., et al. (2016), Effect of ions on sulfuric acid-water binary particle formation: 2. Experimental data and comparison with QC-normalized classical nucleation theory, *J. Geophys. Res. Atmos.*, *121*, 1752–1775, doi:10.1002/2015JD023539.

Ehn, M., et al. (2014), A large source of low-volatility secondary organic aerosol, *Nature*, *506*(7489), 476–479, doi:10.1038/nature13032.

Ehrhart, S., and J. Curtius (2013), Influence of aerosol lifetime on the interpretation of nucleation experiments with respect to the first nucleation theorem, *Atmos. Chem. Phys.*, *13*(22), 11,465–11,471, doi:10.5194/acp-13-11465-2013.

Erupe, M. E., et al. (2010), Correlation of aerosol nucleation rate with sulfuric acid and Ammonia in Kent Ohio: An atmospheric observation, *J. Geophs. Res.*, *115*, D23216, doi:10.1029/2010JD013942.

Glasoe, W. A., K. Volz, B. Panta, N. Freshour, R. Bachman, D. R. Hanson, P. H. McMurry, and C. Jen (2015), Sulfuric acid nucleation: An experimental study of the effect of seven bases, *J. Geophys. Res. Atmos.*, *120*, 1933–1950, doi:10.1002/2014JD022730.

Hanson, D. R., and F. L. Eisele (2000), Diffusion of H_2SO_4 in humidified nitrogen: Hydrated H_2SO_4, *J. Phys. Chem.*, *104*, 1715–1719, doi:10.1021/jp993622j.

Jen, C. N., P. H. McMurry, and D. R. Hanson (2014), Stabilization of sulfuric acid dimers by ammonia, methylamine, dimethylamine, and trimethylamine, *J. Geophys. Res. Atmos.*, *119*, 7502–7514, doi:10.1002/2014JD021592.

Kanawade, V., D. R. Benson, and S. H. Lee (2012), Statistical analysis of 4 year measurements of aerosol sizes in a semi-rural U.S. continental environment, *Atmos. Environ.*, *59*, 30–38, doi:10.1016/j.atmosenv.2012.05.047.

Kirkby, J., et al. (2011), Role of sulphuric acid, ammonia and galactic cosmic rays in atmospheric aerosol nucleation, *Nature*, *476*(7361), 429–433, doi:10.1038/nature10343.

Kontkanen, J., T. Olenius, K. Lehtipalo, H. Vehkamäki, M. Kulmala, and K. E. J. Lehtinen (2016), Growth of atmospheric clusters involving cluster-cluster collisions: Comparison of different growth rate methods, *Atmos. Chem. Phys.*, *16*(9), 5545–5560, doi:10.5194/acp-16-5545-2016.

Kulmala, K., et al. (2013), Direct observations of atmospheric aerosol nucleation, *Science*, *339*(6122), 943–946, doi:10.1126/science.1227385.

Kulmala, M., L. Laakso, K. E. J. Lehtinen, I. Riipinen, M. Dal Maso, A. Lauria, V. M. Kerminen, W. Birmili, and P. H. McMurry (2004), Formation and growth rates of ultrafine atmosphere particles: A review of observations, *J. Aerosol Sci.*, *35*, 143–176.

Kulmala, M., et al. (2012), Measurement of the nucleation of atmospheric aerosol particles, *Nat. Protocols*, *7*(9), 1651–1667, doi:10.1038/nprot.2012.091.

Kupiainen-Määttä, O., T. Olenius, H. Korhonen, J. Malila, M. Dal Maso, K. Lehtinen, and H. Vehkamäki (2014), Critical cluster size cannot in practice be determined by slope analysis in atmospherically relevant applications, *J. Aerosol Sci.*, *77*, 127–144, doi:10.1016/j.jaerosci.2014.07.005.

Kurtén, T., M. Noppel, H. Vehkamäki, M. Salonen, and M. Kulmala (2007), Quantum chemical studies of hydrate formation of H_2SO_4 and HSO_4^-, *Boreal Environ. Res.*, *12*, 431–453.

Larriba, C., C. J. Hogan, M. Attoui, R. Borrajo, J. F. Garcia, and J. F. de la Mora (2011), The mobility–volume relationship below 3.0 nm examined by tandem mobility–mass measurement, *Aerosol Sci. Technol.*, *45*, 453–467, doi:10.1080/02786826.2010.546820.

Lehtipalo, K., et al. (2014), Methods for determining particle size distribution and growth rates between 1 and 3 nm using the particle size magnifier, *Boreal Environ. Res.*, *19*, 215–236.

Lehtipalo, K., et al. (2016), The effect of acid–base clustering and ions on the growth of atmospheric nano-particles, *Nat. Commun.*, *7*, 11,594, doi:10.1038/ncomms11594.
Leppä, J., T. Anttila, V. M. Kerminen, M. Kulmala, and K. E. J. Lehtinen (2011), Atmospheric new particle formation: Real and apparent growth of neutral and charged particles, *Atmos. Chem. Phys.*, *11*(10), 4939–4955, doi:10.5194/acp-11-4939-2011.
Merikanto, J., D. V. Spracklen, G. W. Mann, S. J. Pickering, and K. S. Carslaw (2009), Impact of nucleation on global CCN, *Atmos. Chem. Phys.*, *9*, 8601–8616, doi:10.5194/acp-9-8601-2009.
Merikanto, J., J. Duplissy, A. Määttänen, H. Henschel, N. M. Donahue, D. Brus, S. Schobesberger, M. Kulmala, and H. Vehkamäki (2016), Effect of ions on sulfuric acid-water binary particle formation: 1. Theory for kinetic- and nucleation-type particle formation and atmospheric implications, *J. Geophys. Res. Atmos.*, *121*, 1736–1751, doi:10.1002/2015JD023538.
Neitola, K., D. Brus, U. Makkonen, M. Sipilä, R. L. Mauldin Iii, N. Sarnela, T. Jokinen, H. Lihavainen, and M. Kulmala (2015), Total sulfate vs. sulfuric acid monomer concentrations in nucleation studies, *Atmos. Chem. Phys.*, *15*(6), 3429–3443, doi:10.5194/acp-15-3429-2015.
Nieminen, T., K. E. J. Lehtinen, and M. Kulmala (2010), Sub-10 nm particle growth by vapor condensation—Effects of vapor molecule size and particle thermal speed, *Atmos. Chem. Phys.*, *10*(20), 9773–9779, doi:10.5194/acp-10-9773-2010.
Seinfeld, J. H., and S. N. Pandis (2006), *Atmospheric Chemistry and Physics: From Air Pollution to Climate Change*, 2nd ed., John Wiley, New York.
Sipila, M., et al. (2010), The role of sulfuric acid in atmospheric nucleation, *Science*, *327*, 1243–1246, doi:10.1126/science.1180315.
Skrabalova, L., D. Brus, T. Anttila, V. Zdimal, and H. Lihavainen (2014), Growth of sulphuric acid nanoparticles under wet and dry conditions, *Atmos. Chem. Phys.*, *14*(12), 6461–6475, doi:10.5194/acp-14-6461-2014.
Stolzenburg, M. R., P. H. McMurry, H. Sakurai, J. N. Smith, R. L. Mauldin, F. L. Eisele, and C. F. Clement (2005), Growth rates of freshly nucleated atmospheric particles in Atlanta, *J. Geophys. Res.*, *110*, D22S05, doi:10.1029/2005JD005935.
Tröstl, J., et al. (2016), The role of low-volatility organic compounds in initial particle growth in the atmosphere, *Nature*, *533*, doi:10.1038/nature18271.
Vaida, V. (2011), Perspective: Water cluster mediated atmospheric chemistry, *J. Chem. Phys.*, *135*(2), 020,901, doi:10.1063/1.3608919.
Vanhanen, J., J. Mikkila, K. Lehtipalo, M. Sipila, H. E. Manninen, E. Siivola, T. Petaja, and M. Kulmala (2011), Particle size magnifier for Nano-CN detection, *Aerosol Sci. Technol.*, *45*(4), 533–542, doi:10.1080/02786826.2010.547889.
Vehkamäki, H., M. Kulmala, I. Napari, E. J. Lehtinen, C. Timmreck, M. Noppel, and A. Laaksonen (2002), An improved parameterization for sulfuric acid-water nucleation rates for tropospheric and stratospheric conditions, *J. Geophys. Res.*, *107*(D22), 4622, doi:10.1029/2002JD002184.
Wimmer, D., et al. (2015), Technical note: Using deg-cpcs at upper tropospheric temperatures, *Atmos. Chem. Phys.*, *15*(13), 7547–7555, doi:10.5194/acp-15-7547-2015.
Wyslouzil, B. E., J. H. Seinfeld, R. C. Flagan, and K. Okuyama (1991), Binary nucleation in acid-water systems. II Sulphuric acid-water and a comparison with methanesulphonic acid-water, *J. Chem. Phys.*, *94*, 6842–6850, doi:10.1063/1.460262.
Young, L. H., D. R. Benson, F. Rifkha, J. R. Pierce, H. Junninen, M. Kulmala, and S.-H. Lee (2008), Laboratory studies of sulfuric acid and water binary homogeneous nucleation: Evaluation of laboratory setup and preliminary results, *Atmos. Chem. Phys.*, *8*, 1–20, doi:10.5194/acp-8-4997-2008.
Yu, F. (2002), Altitude variations of cosmic ray induced production of aerosols: Implication on global cloudiness and climate, *J. Geophys. Res.*, *107*(A7), 1118, doi:10.1029/2001JA000248.
Yu, F., and G. Luo (2009), Simulation of particle size distribution with a global aerosol model: contribution of nucleation to aerosol and CCN number concentrations, *Atmos. Chem. Phys.*, *9*(20), 7691–7710, doi:10.5194/acp-9-7691-2009.
Yu, H., R. McGraw, and S.-H. Lee (2012), Effects of amines on formation of sub-3 nm particles and their subsequent growth, *Geophys. Res. Lett.*, *39*, L02807, doi:10.1029/2011GL050099.
Yu, H., L. Zhou, L. Dai, W. Shen, W. Dai, J. Zheng, Y. Ma, and M. Chen (2016), Nucleation and growth of sub-3 nm particles in the polluted urban atmosphere of a megacity in China, *Atmos. Chem. Phys.*, *16*(4), 2641–2657, doi:10.5194/acp-16-2641-2016.
Zhang, R., A. Khalizov, L. Wang, M. Hu, and W. Xu (2012), Nucleation and growth of nanoparticles in the atmosphere, *Chem. Rev.*, *112*(3), 957–2011.
Zollner, J. H., W. A. Glasoe, B. Panta, K. K. Carlson, P. H. McMurry, and D. R. Hanson (2012), Sulfuric acid nucleation: Power dependencies, variation with relative humidity, and effect of bases, *Atmos. Chem. Phys.*, *12*, 4399–4411, doi:10.5194/acp-12-4399-2012.